Anisotropic encoding of three-dimensional space by place cells and grid cells

Hayman, R., Verriotis, M.A., Jovalekic, A. , Fenton, A.A., and Jeffery, K.J.

Supplementary information

Supplementary Figure 1 The recording apparatus. (a) Photograph of the pegboard, on which a tethered rat is exploring. (b) Photograph of the helical track. (c) Sections of a typical path on the pegboard showing that the rats tended to run diagonally, but not in a regular and stereotyped way. The sections of this run have been selected to start (green arrow) and stop (red arrow) at the point where the rat turned around on the apparatus. The small red dots show spikes from a grid cell. The complete trial (in this case, shorter than usual, hence the bias to one side) is shown on the right.

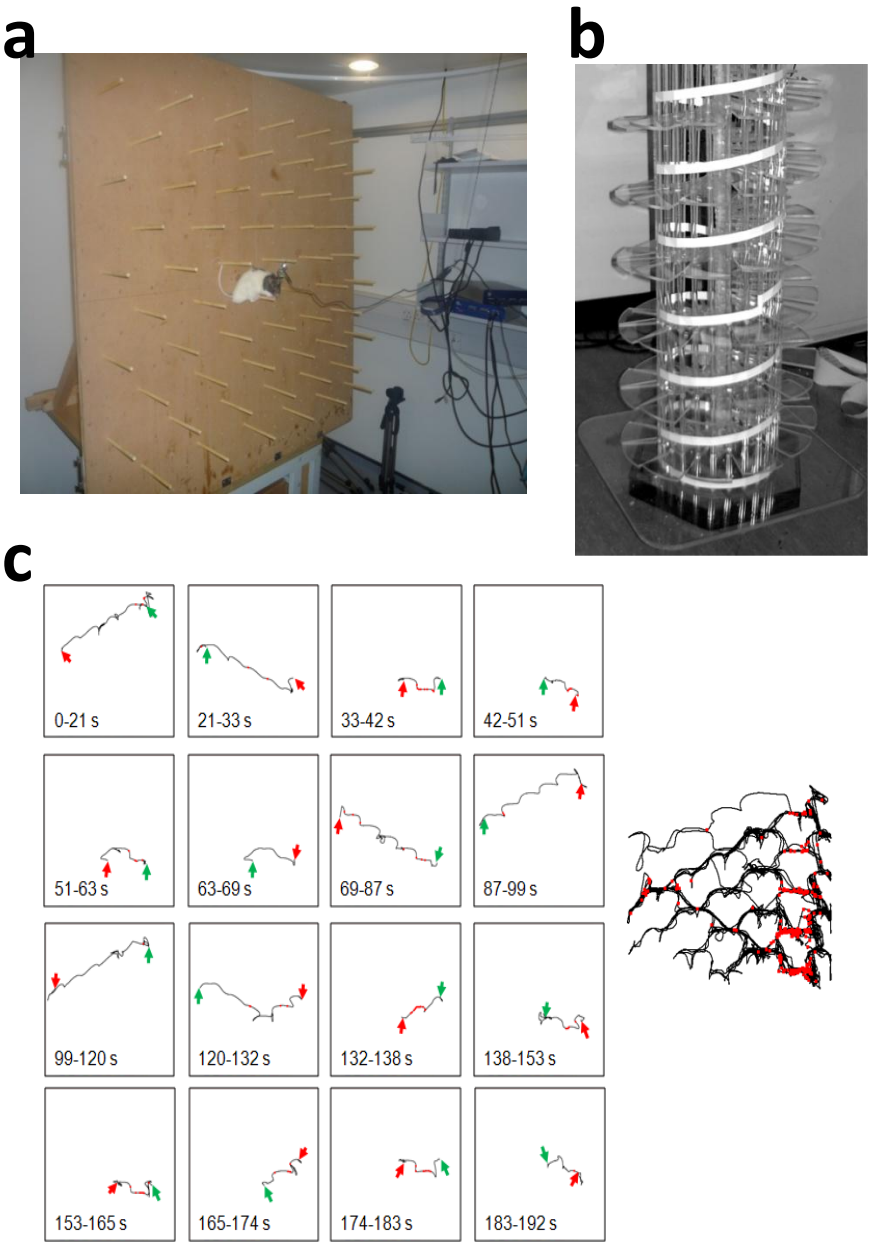

Nature Neuroscience: doi:10.1038/nn.2892

Supplementary Figure 2 (3 pages) Firing characteristics of the complete set of place cells recorded on the pegboard arena. Each cell's data are plotted as follows: Left top: Spike plots for place cells on the open field, showing position (black lines) with spikes superimposed (blue squares). Left bottom: Same data re-plotted as firing rate maps, depicted as described in the Fig. 1 legend. Middle column: Spike plots for place cells on the pegboard arena, showing position (black lines) with spikes superimposed (blue squares). Right column: Same data re-plotted as firing rate maps.

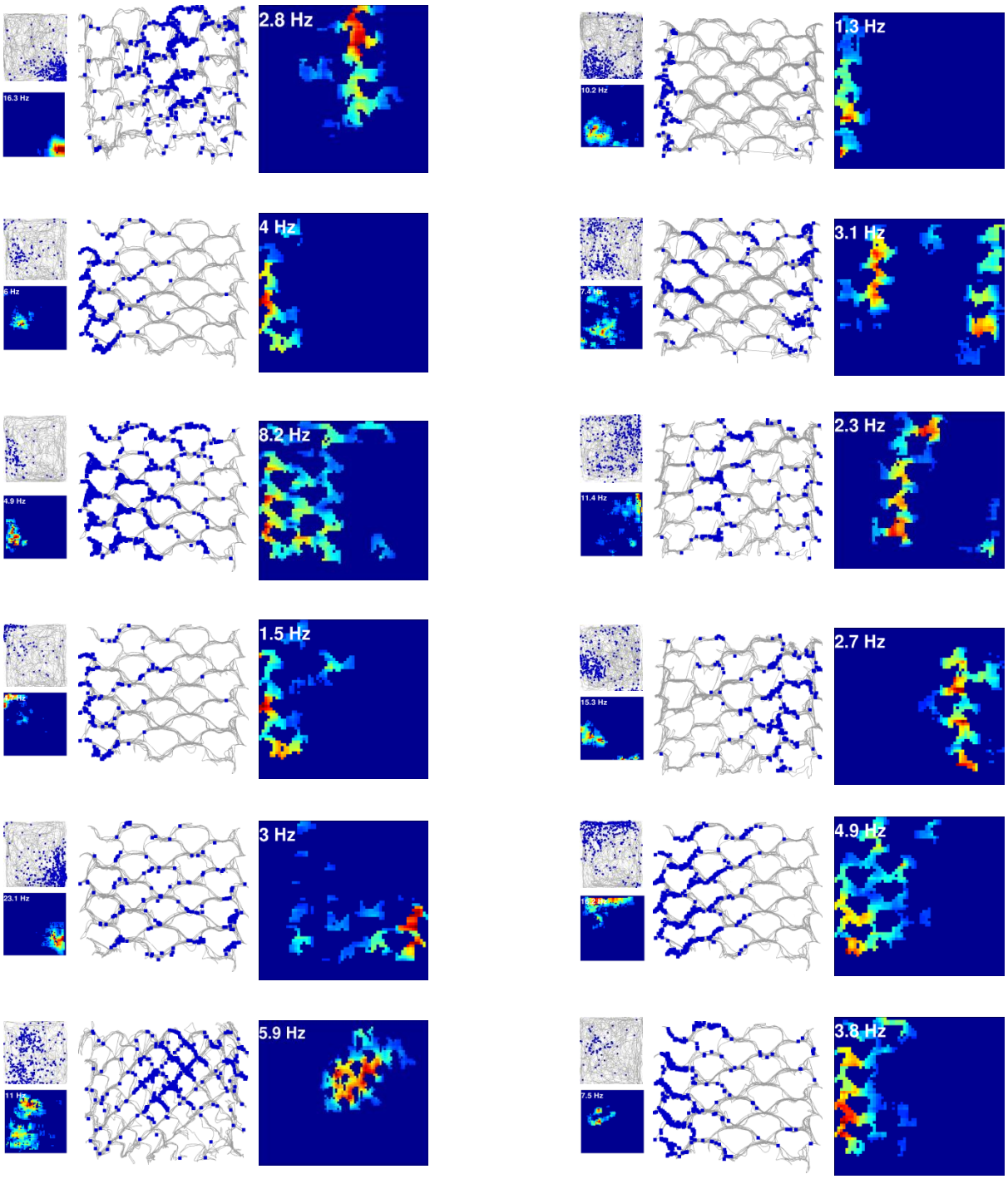

Nature Neuroscience: doi:10.1038/nn.2892

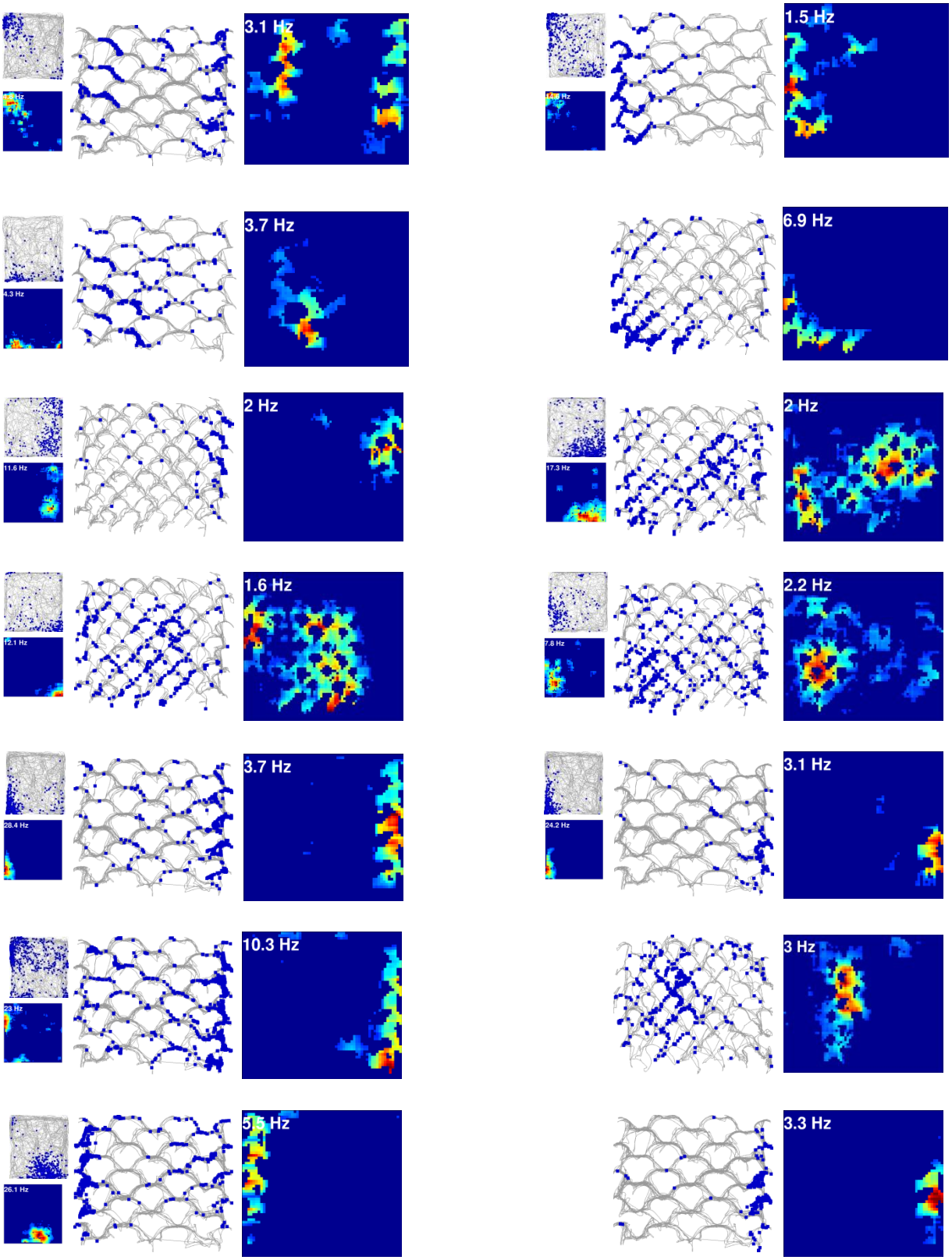

Nature Neuroscience: doi:10.1038/nn.2892

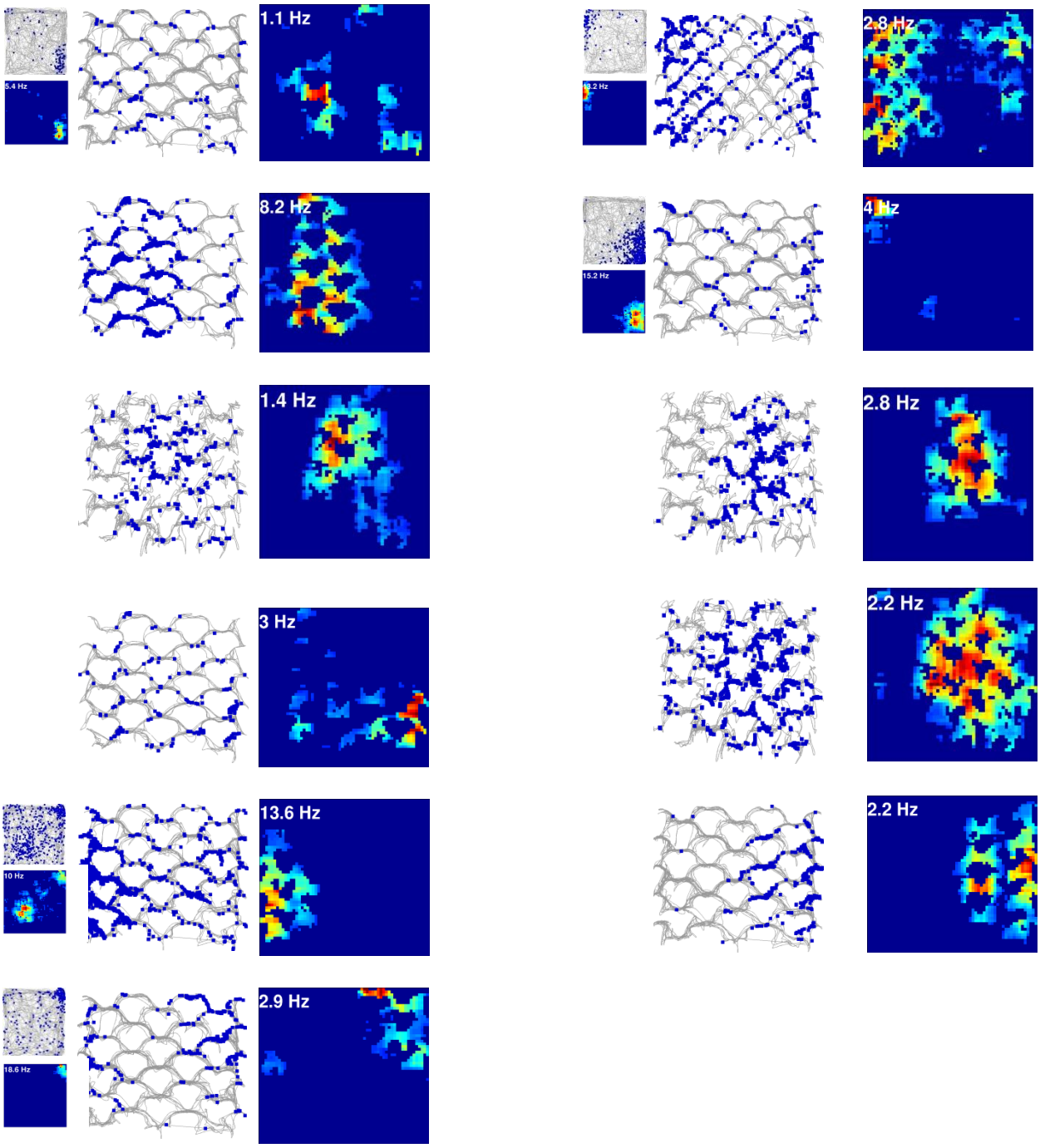

Nature Neuroscience: doi:10.1038/nn.2892

Supplementary Figure 3 Firing rate with respect to distance from the field peak (in layers, for the pegboard, or coils, for the helix). For the helical track, the dummy cell data are also shown. Note that these plots exclude the peak itself, which by definition had the highest firing rate: nevertheless, firing continued to fall steadily with distance, rather than fluctuating randomly, suggesting a systematic modulation of firing rate by height cues.

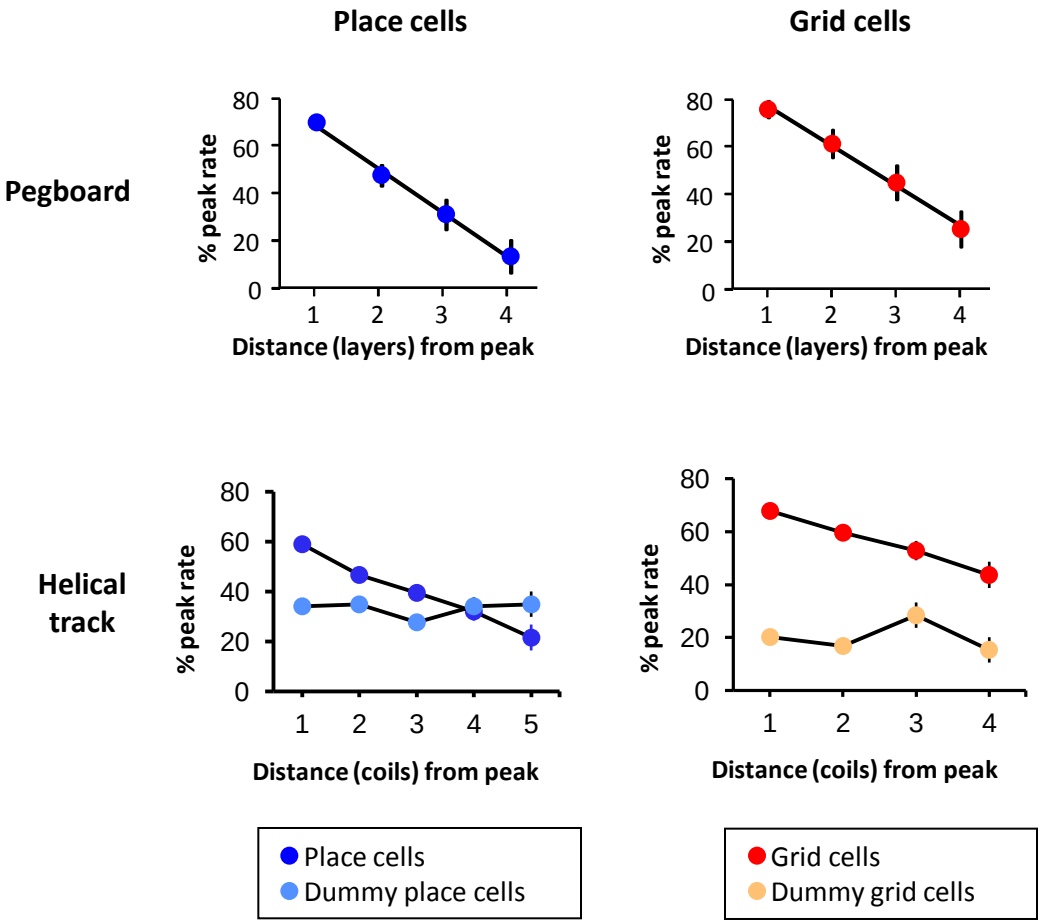

Nature Neuroscience: doi:10.1038/nn.2892

Supplementary Figure 4 (4 pages) Data for the complete set of grid cells recorded on the flat arenas (a-d) or the pegboard (e-h). For the spike plots (a and e), spikes are shown in red and the path of the rat is shown in black. Rate maps (b and f) are smoothed, contour-plotted version of the spike plots, showing hot-spots of activity corresponding to the firing fields. Peak rates (Hz) are shown in white text. Spatial autocorrelograms of the firing fields (c and g) show a predominantly hexagonal close-packed pattern for recordings in the flat arenas (c), and a striped pattern for recordings on the pegboard (g). Symmetry plots (d and h; see Supplementary methods for details) showed a predominantly 6-peaked pattern for the flat arenas (d) and a two-peaked pattern on the pegboard (h).

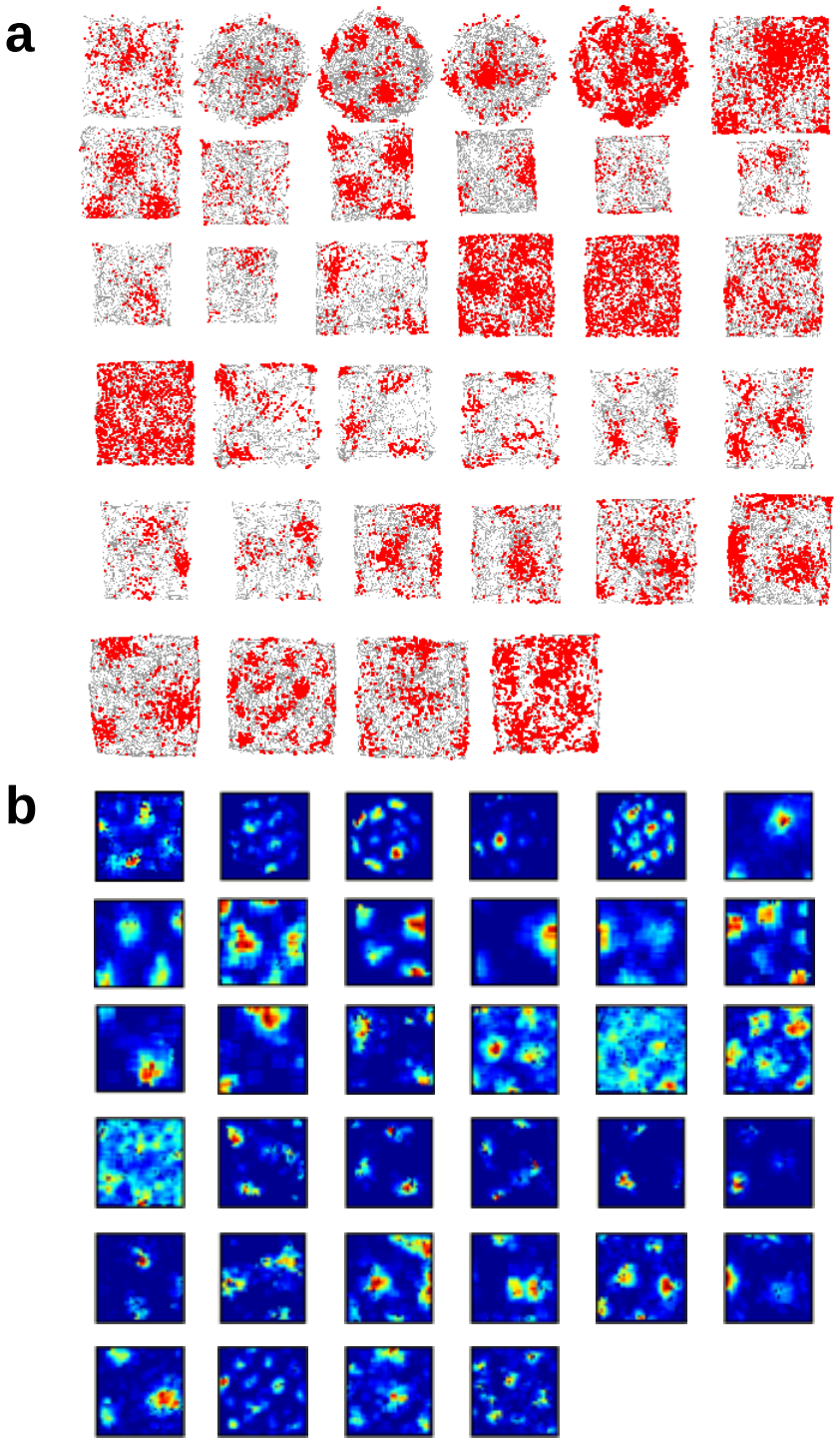

Nature Neuroscience: doi:10.1038/nn.2892

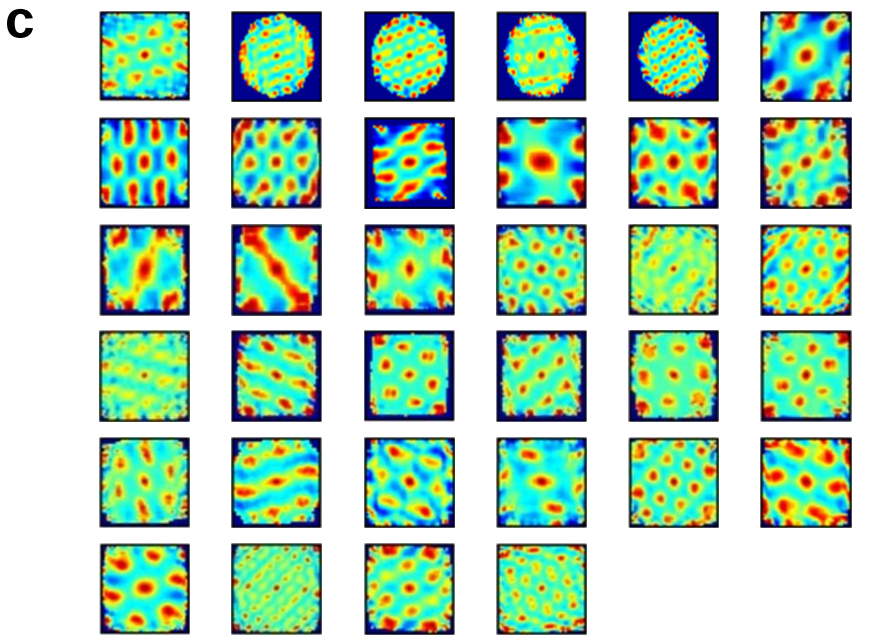

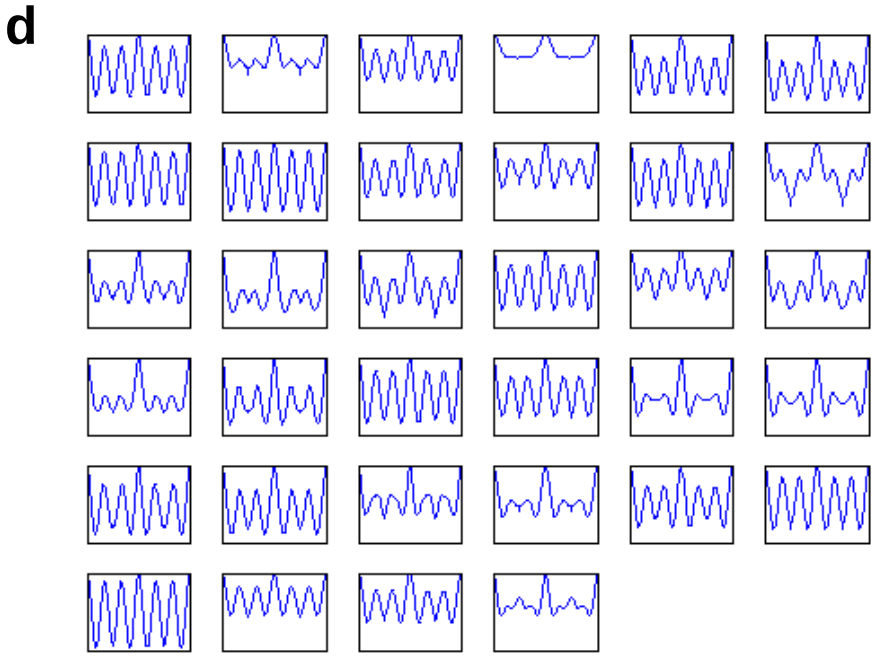

Nature Neuroscience: doi:10.1038/nn.2892

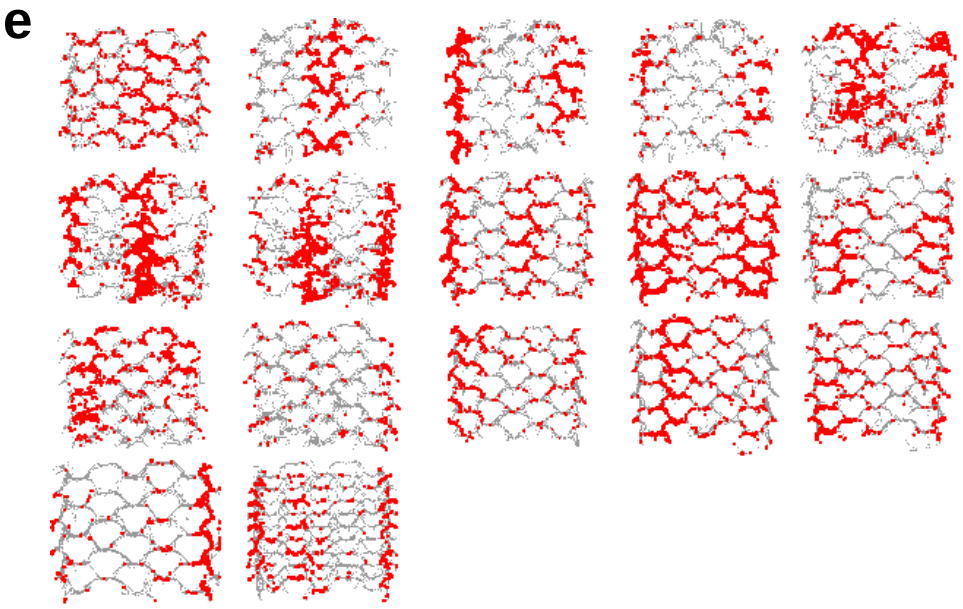

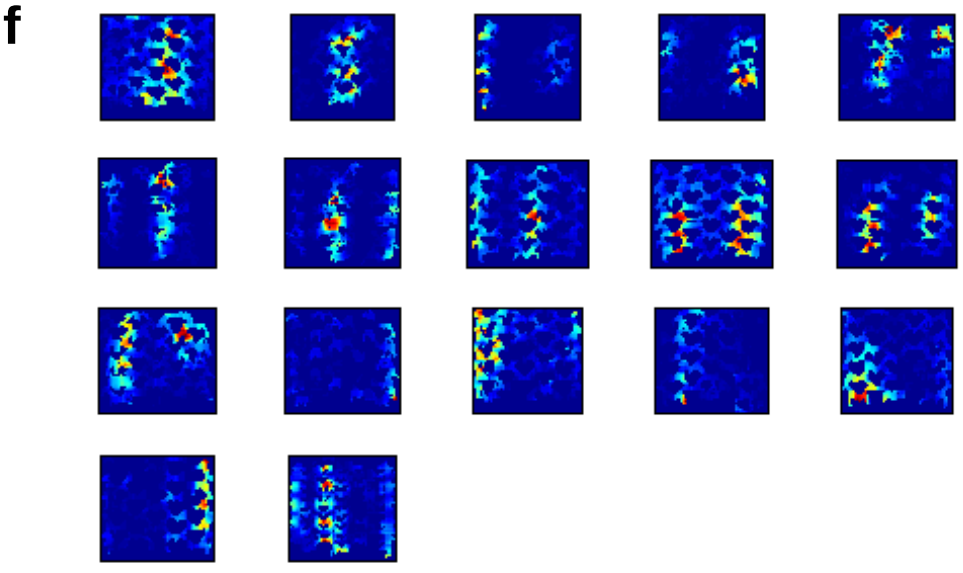

Nature Neuroscience: doi:10.1038/nn.2892

g

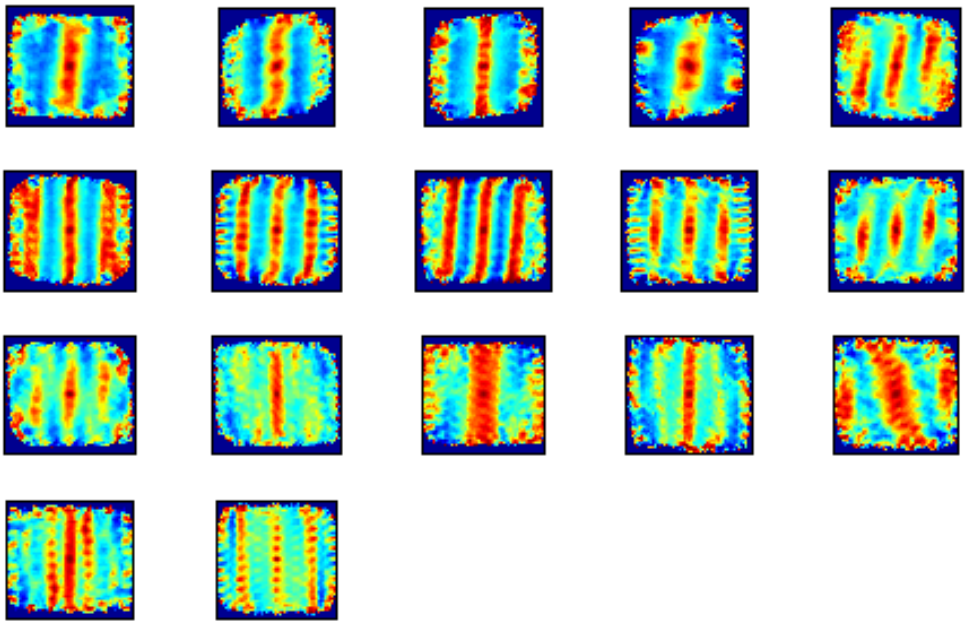

h

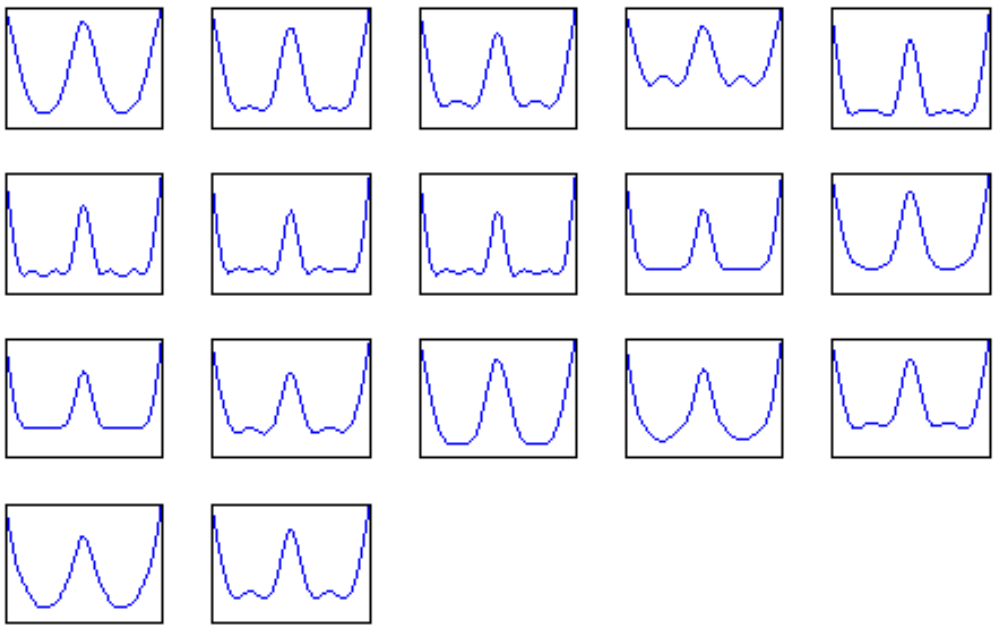

Nature Neuroscience: doi:10.1038/nn.2892

Supplementary Figure 5 Symmetry analyses for grid cells on flat arenas vs. the pegboard. (a) Rotational symmetry analysis. From top to bottom are: raw data from 2 cells, corresponding firing rate contour plots, spatial autocorrelation maps (black Xs mark peaks, red Xs mark peaks for the corresponding flat trial, for comparison) and rotational autocorrelation plots. Lowermost plots show population rotational symmetry plots (black line = mean, green = 95% confidence limits). (b) Mean (+/- s.e.m.) symmetry plot peaks for grid cells recorded on the flat arenas (light red) or pegboard (dark red), calculated for a range of peak-trough thresholds. (c) Histogram of translational symmetry (means +/- s.e.m).

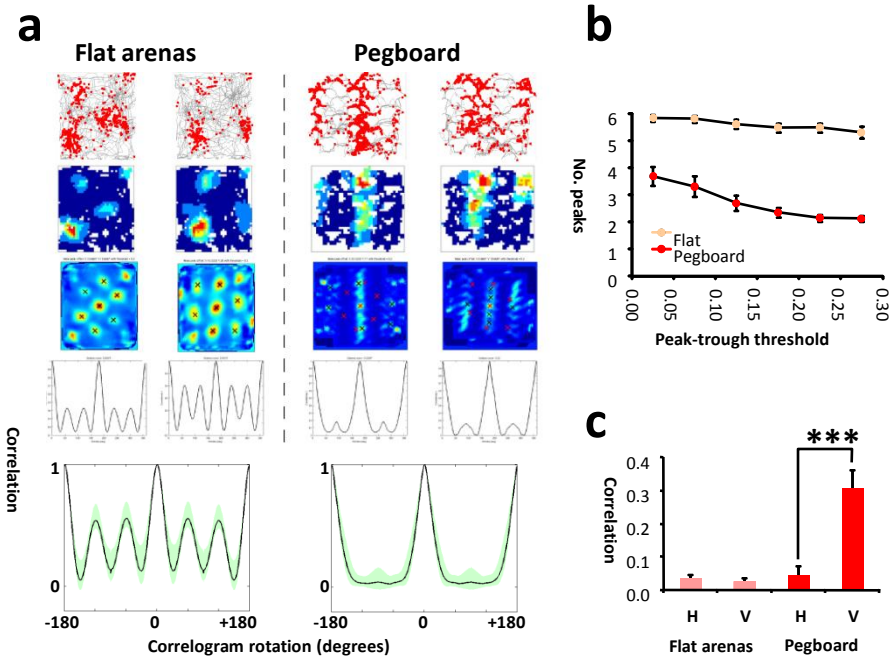

Supplementary Figure 6 Spike plots (left panels) and firing rate maps (right panels), for four grid cells recorded on the pegboard when it was laid in a horizontal position, showing a clear grid structure.

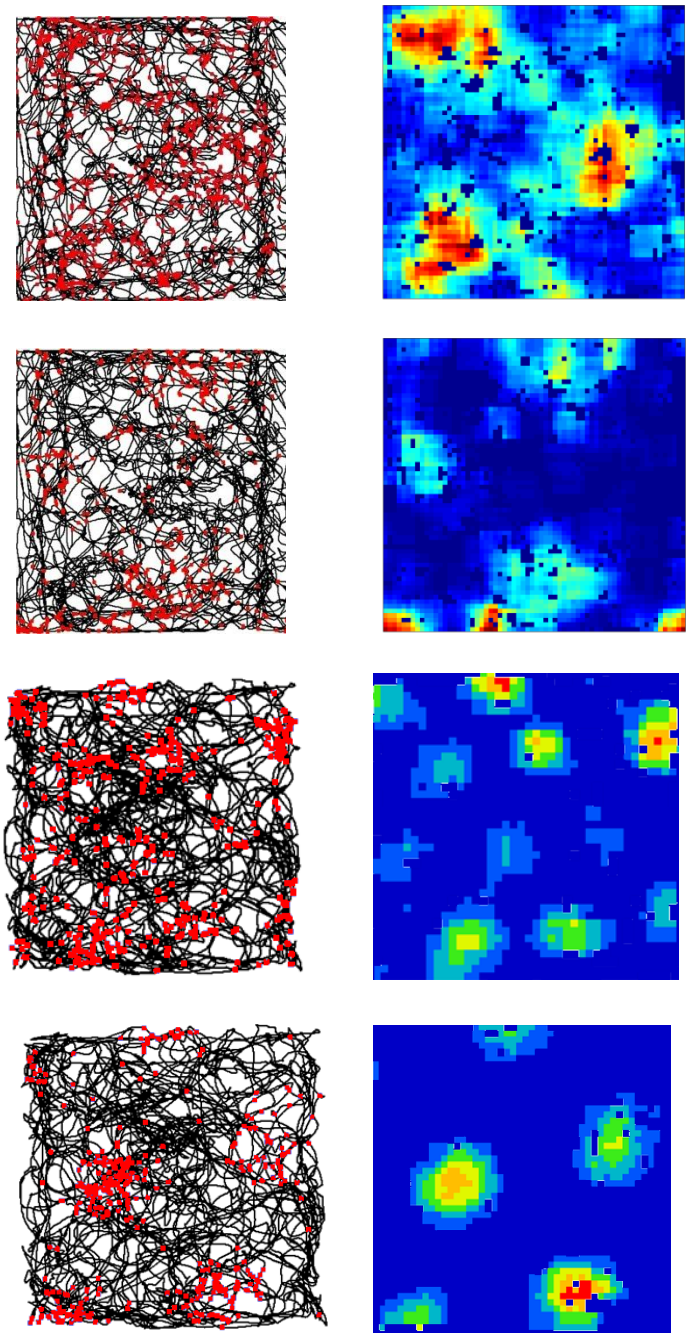

Nature Neuroscience: doi:10.1038/nn.2892

Supplementary Figure 7 Firing rate maps from the 17 pegboard grid cells, decomposed into up-going, down-going, and left- and right-going trial segments. The stripe pattern persisted regardless of travel direction.



Nature Neuroscience: doi:10.1038/nn.2892

Supplementary Figure 8 Comparison of firing fields on the flat arenas (left of each pair) vs. pegboard for the 16 grid cells that were recorded on both types of apparatus. Note that in no cases is the stripe width on the pegboard less than the inter-field distance on the flat arena.

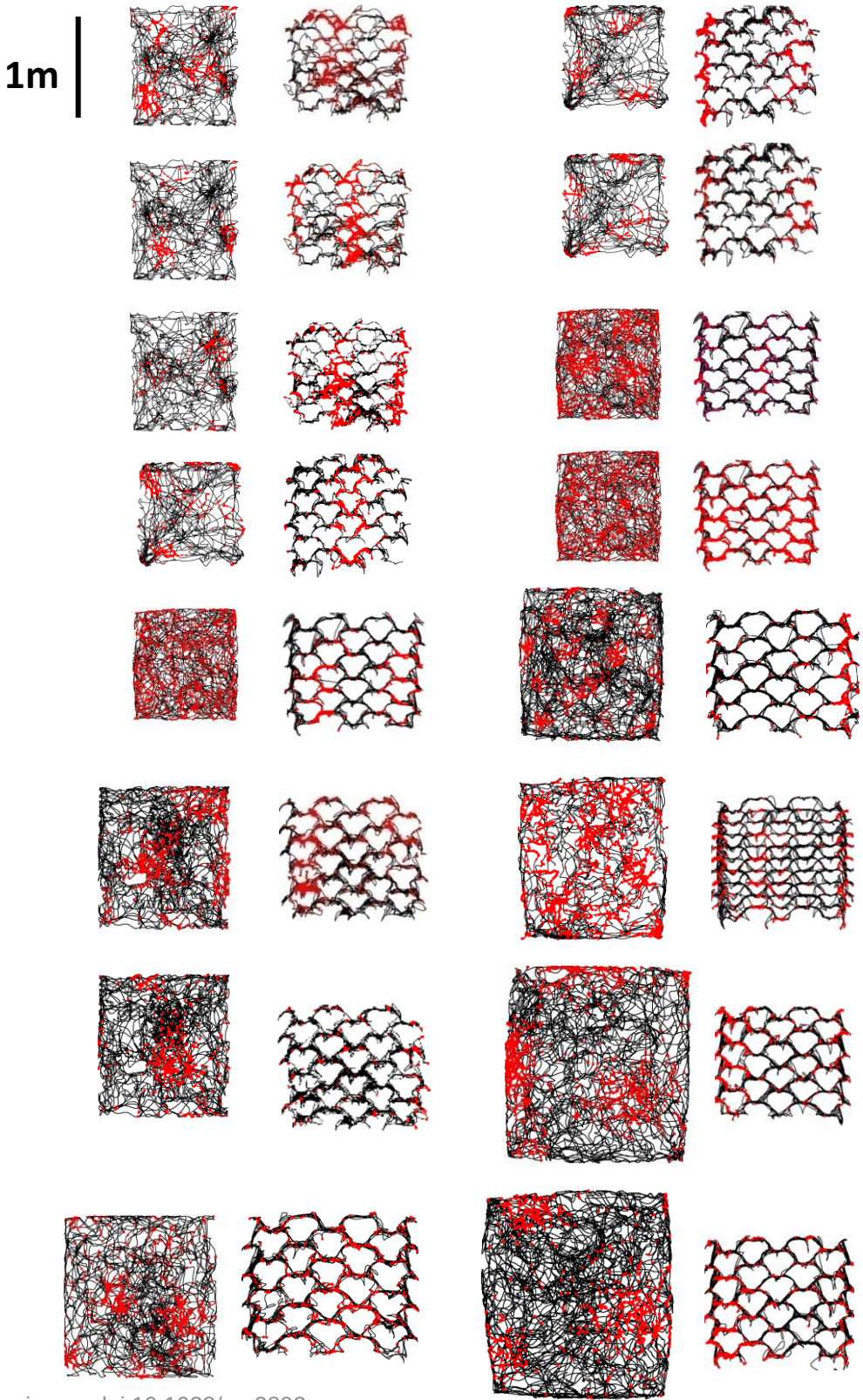

Nature Neuroscience: doi:10.1038/nn.2892

Supplementary Figure 9 Procedure for analyzing spatial firing on the helical track. (a) Each run was divided into its component 5 (in this case) or 6 coils. This was done independently for upward (shown here; 5 runs from bottom to top in this example) and downward runs. (b) Each coil was unwound into a linear plot and divided into 64 bins, and firing was plotted as firing rate histograms (i.e., number of spikes in each bin normalized by dwell time), stacked on top of each other. Numbers below each firing rate histogram indicate the coil number, with coil 1 at the bottom and coil 5 (in this case) or 6 at the top. The linearized plots in (b) were labelled according to distance from the peak rate coil: the peak rate coil was coil 0, and coils below were incremented positively, in either direction .

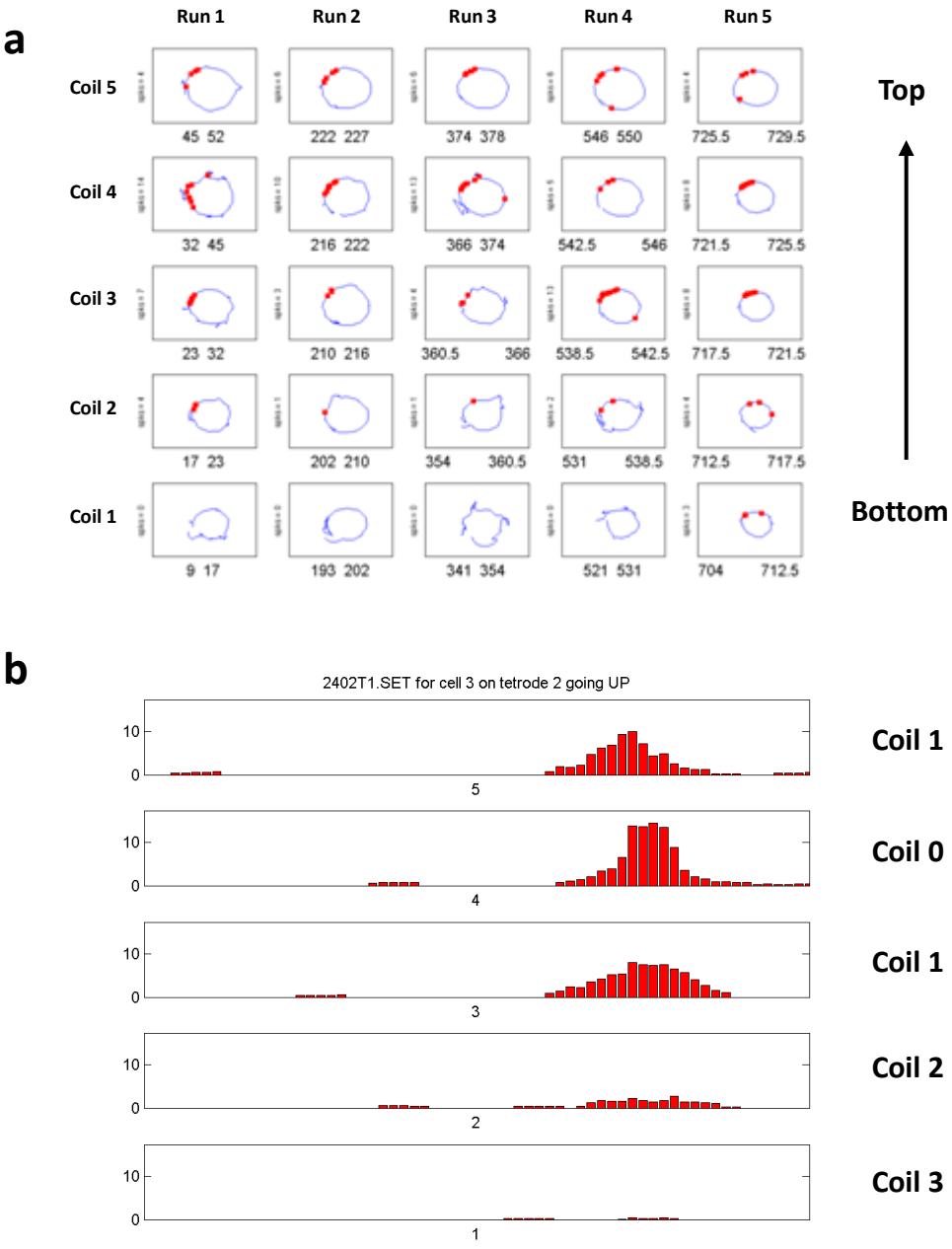

Supplementary Figure 10 (2 pages) The complete set of place fields recorded on the helical track. Data are separated into up-going and down-going runs. Note that firing tended to be localized in a particular region of each segment, and furthermore, that this region was the same on successive coils. Thus, there is no evidence of positional remapping. However, a number of cells (outlined in bold) showed rate modulation, inasmuch as the firing rate declined across coils at every step of the way.

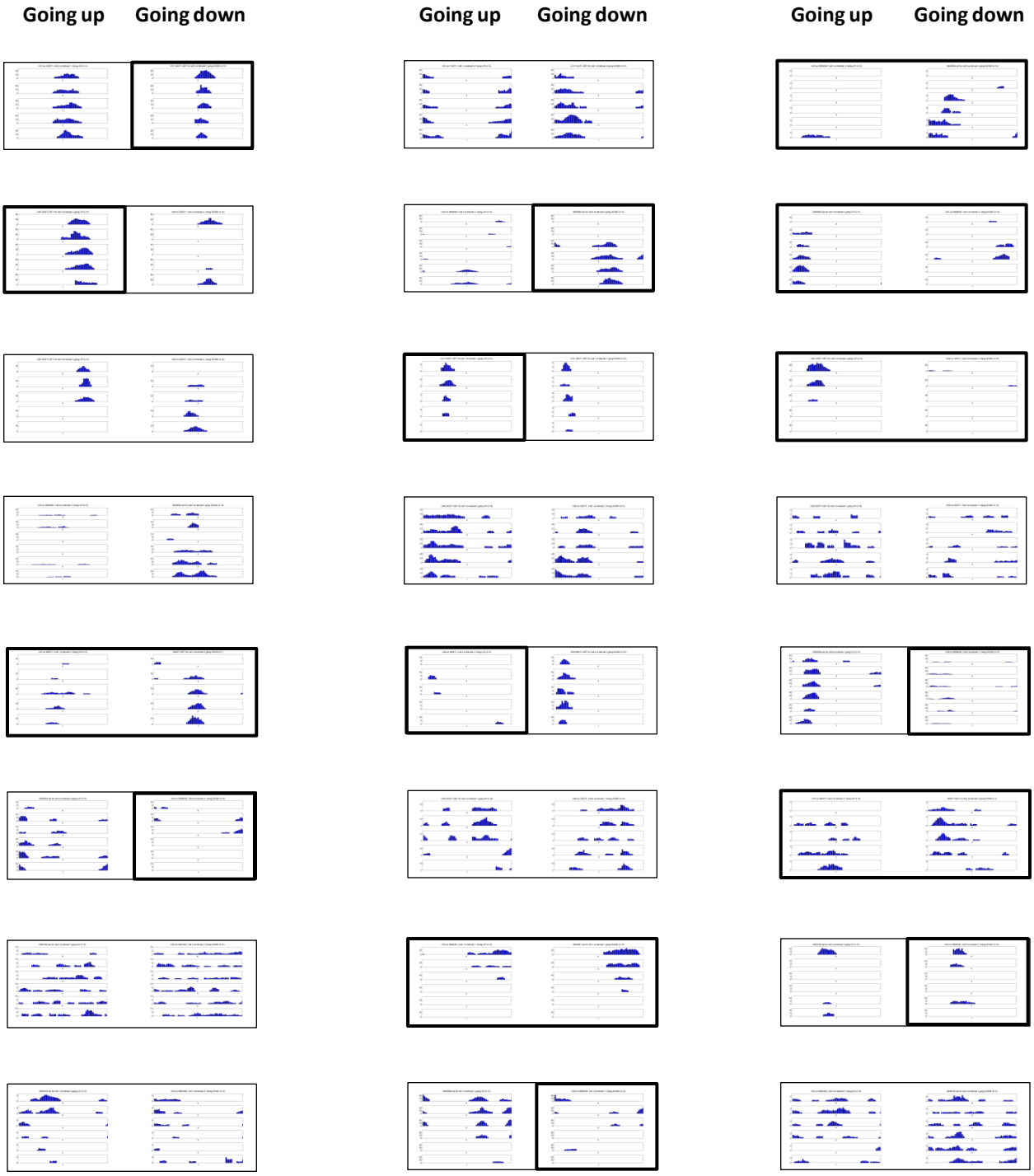

Nature Neuroscience: doi:10.1038/nn.2892

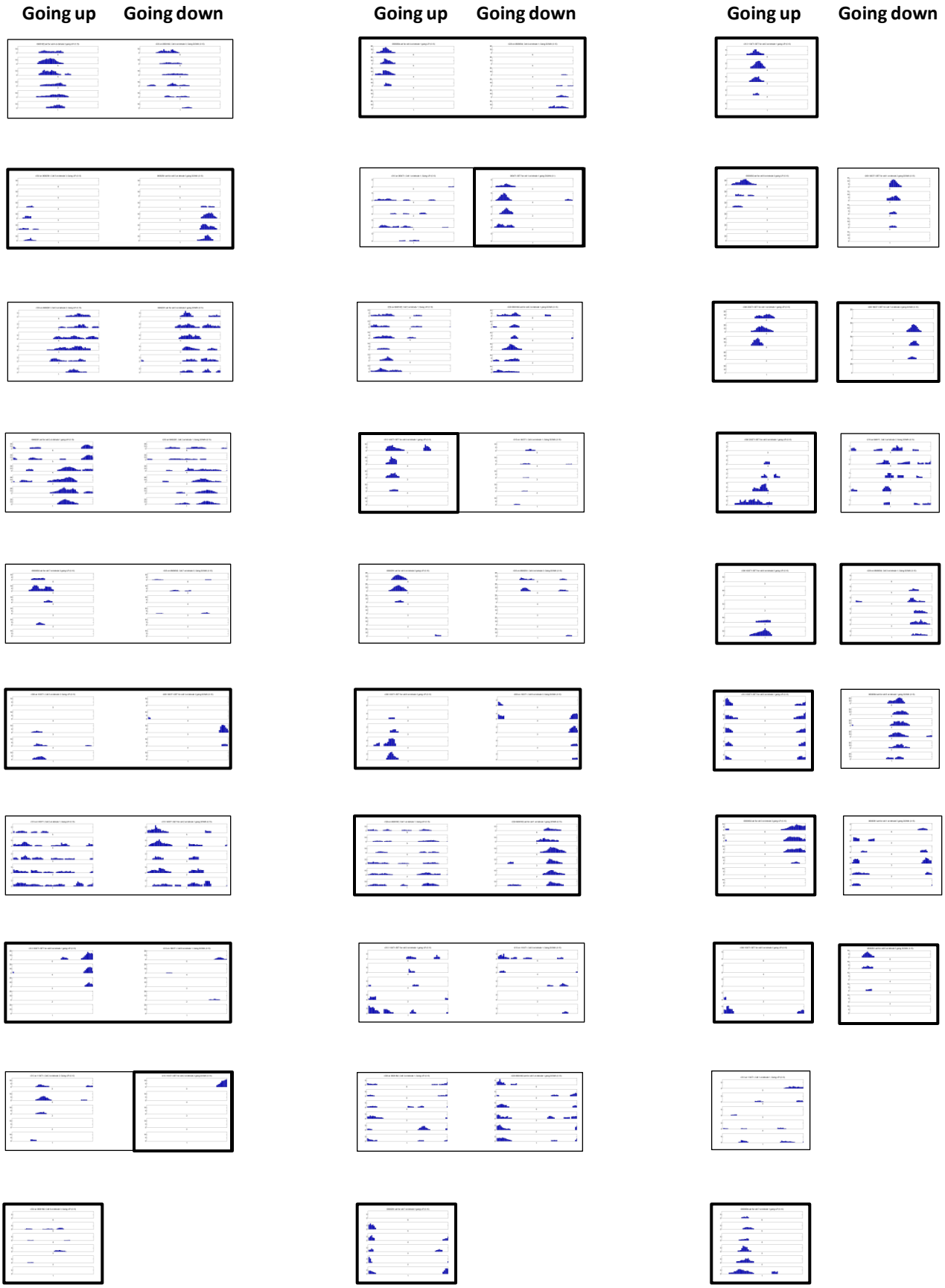

Nature Neuroscience: doi:10.1038/nn.2892

Supplementary Figure 11 Distribution of firing field peaks on the helical track. Upper graphs show place cells recorded on either the 5-coil or 6-coil configuration of the track, separated into up-going and down-going directions. Lower graphs show primary or secondary grid cell fields, also separated into up-going or down-going runs. There is no consistent tendency for field peaks to cluster at any particular level of the helix, in either the up-going or down-going directions.

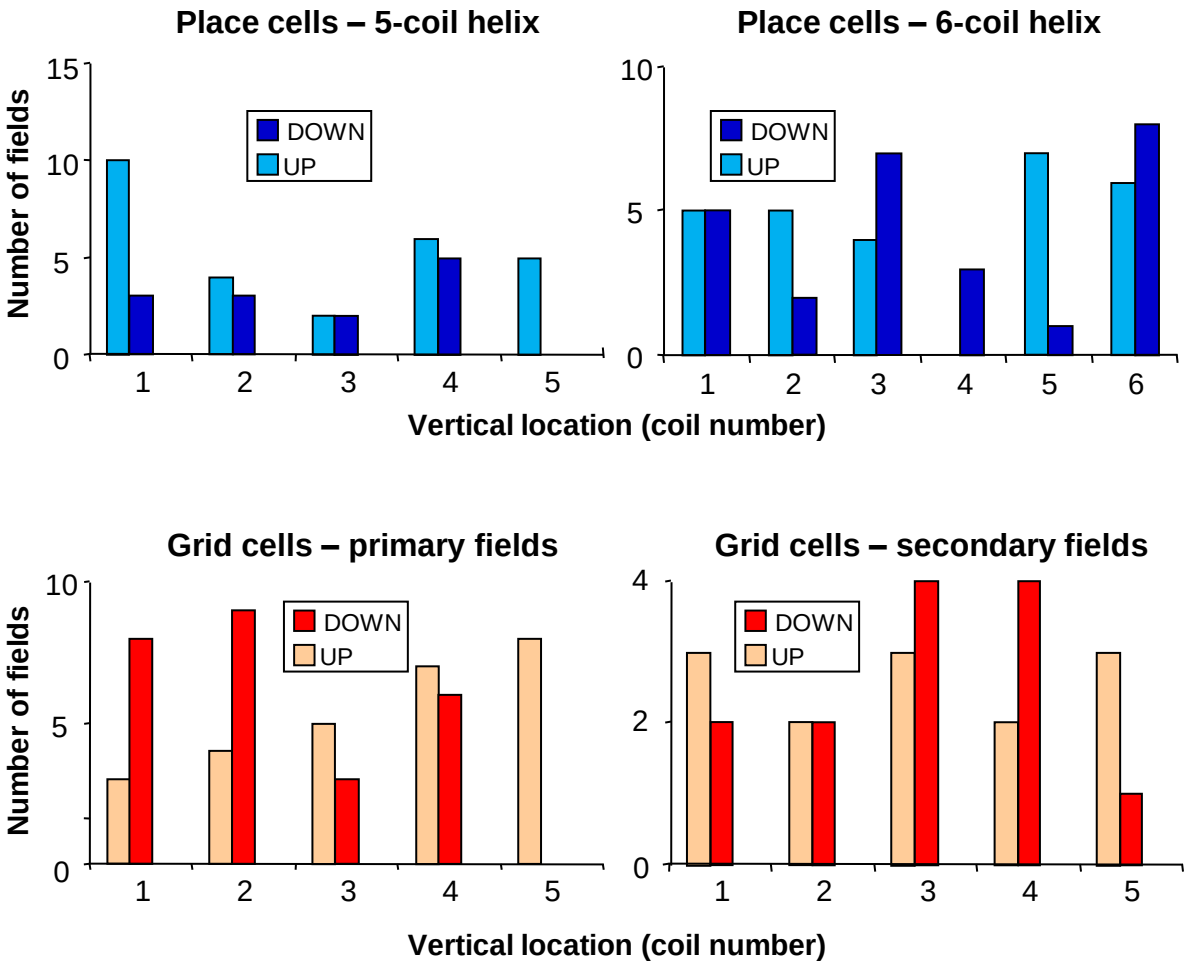

Supplementary Figure 12 The complete set of grid fields recorded on the helical track. Data are depicted as shown in Supplementary figure 2 and Supplementary figure 9. Note that as with place cells, firing tended to be localized in a particular region of each segment, but unlike the place cells there was usually more than one firing location on a given coil. Firing locations were generally the same on successive coils. Some cells (outlined in bold for primary fields only) showed rate modulation, where firing rate declined across coils at every step of the way, but this occurred far less often than with the place cells (18/79 (23%) of the grid fields, including the secondary fields which have not been highlighted in the figure, compared with 53/103 (51%) of the place fields.



Supplementary Figure 13 (2 pages) Histological sections from 7 of the 10 rats in which grid cells were obtained (in the remaining 3 rats, the electrode track could not be identified). Each set shows (left) a low-power view of the section in which the electrode track was found (red dot indicates estimated site of electrode tip, rectangle shows area that was magnified) and (right) a high power view of the electrode track area. Estimated electrode tip sites: 216 and 245 = Deep layers of either medial entorhinal cortex (MEC) or parasubiculum (PaS), 255 = MEC, 262 = border of PaS and MEC, 323 = layer II of MEC and layer V/VI of MEC/PaS (two tracks), 352 = layer III of either MEC or PaS, 363 = subiculum/dentate molecular layer.

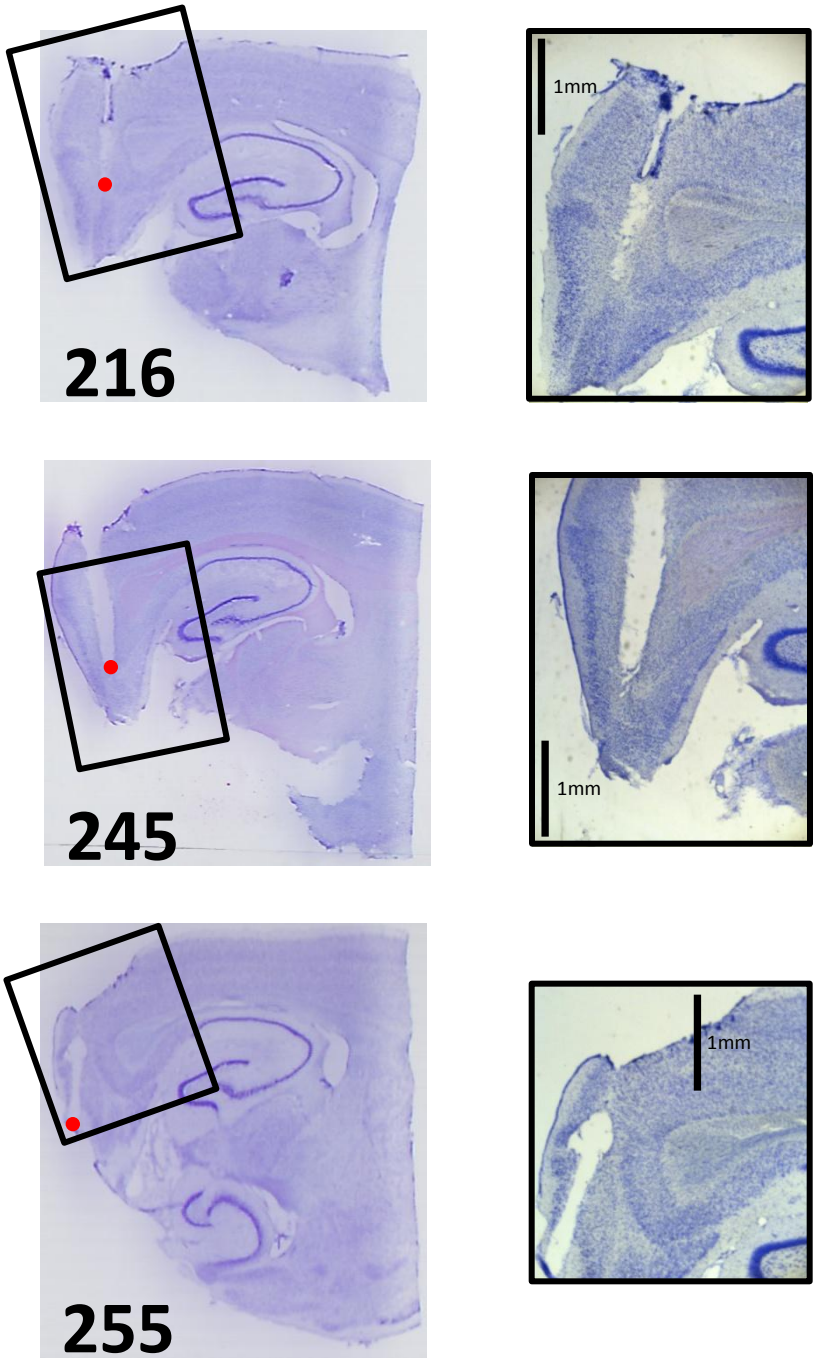

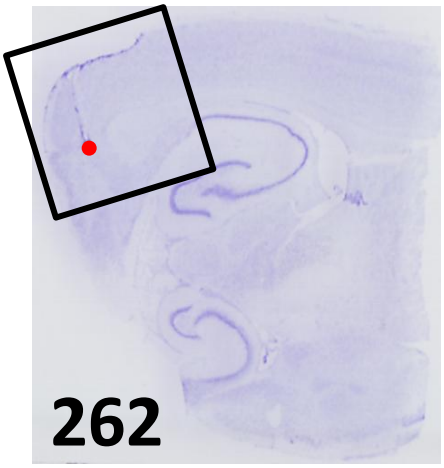

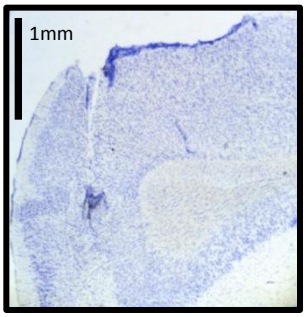

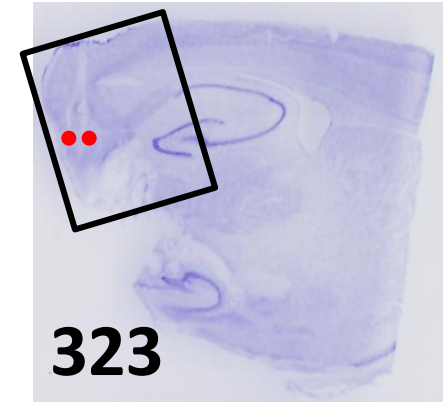

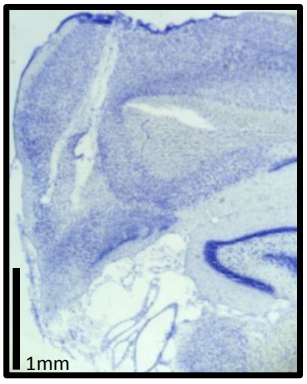

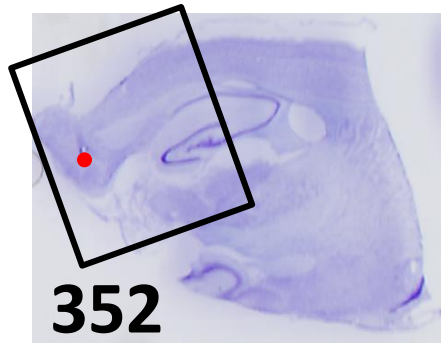

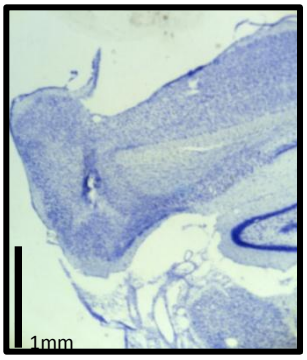

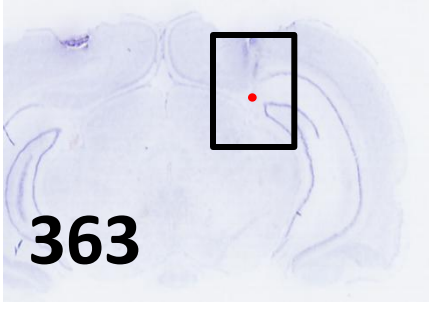

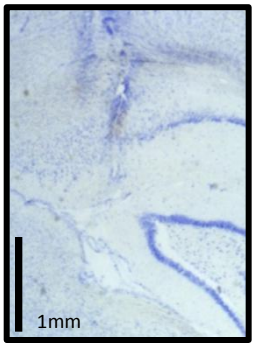

Nature Neuroscience: doi:10.1038/nn.2892

Supplementary results

We recorded 53 place cells and 34 grid cells on flat arenas, 40 place cells and 17 grid cells on the pegboard arena, and 61 place cells and 27 grid cells on the helical track. The complete place cell data set on the pegboard is shown in supplementary figure 3, and for the grid cells in supplementary figure 4. For the data described below, means +/- s.e.m. are reported throughout, except where otherwise specified.

Pegboard

Most of the pegboard analyses are detailed in the main text. However, we also performed an additional analysis, of "symmetry class", to further characterize the differences between horizontal and vertical firing field properties.

Grid field symmetry class

We used two symmetry analyses, one translational and one rotational. Each analysis comprised a double autocorrelation procedure, adapted from the methods of Hafting et al.[3] and Sargolini et al.[22], in which a spatial autocorrelogram, generated from the firing rate map, was rotated or translated (with no wraparound) and re-correlated with the original autocorrelogram at each step. For the rotational analysis the resulting values were plotted and the major peaks determined by counting peaks above a threshold peak-trough correlation difference, for thresholds ranging from 0.0 to 0.3 (Supplementary figure 5). The horizontal ratemaps generally produced six-peaked symmetry plots (mean peak number ranging from 5.82+/-0.13 to 5.29+/-0.22) whereas the pegboard plots were usually two-peaked, reflecting the two-fold symmetry of the stripes, (mean peak number ranging from 3.68+/-0.35 to 2.12+/-0.12).

Nature Neuroscience: doi:10.1038/nn.2892

Chi-square analysis of plots having 2, 4 and 6 peaks for the flat vs. pegboard conditions was highly significant both for threshold=0.0 ($\chi^2(2, N=50)=29.6$, $p<0.0001$) and threshold=0.3 ($\chi^2(2, N=51)=30.0$, $p<0.0001$). Thus, firing patterns on the flat arenas had a different order of rotational symmetry from firing patterns on the pegboard.

For the translational analysis, the values generated by the re-correlations were averaged, for translations in orthogonal directions (horizontal and vertical for the pegboard maps, arbitrarily chosen “horizontal” and “vertical” for the flat maps). The flat maps produced low correlations in both translation directions, of 0.032+/-0.011 and 0.022+/-0.012 for “horizontal” and “vertical”, respectively. On the pegboard, horizontal translation also produced a low correlation of 0.044+/-0.027. By contrast, vertical translation correlations averaged 0.304+/-0.057. A two-factor ANOVA of environment type against translation direction showed a significant effect of environment [$F_{(1,64)}=21.3$, $p<0.001$], a significant effect of translation direction [$F_{(1,64)}=13.7$, $p<0.001$] and a significant interaction [$F_{(1,64)}=18.2$, $p<0.001$]. Post-hoc Tukey’s analysis confirmed that the vertical correlation mean on the pegboard was higher than the horizontal ($t_{(32)}=4.15$, $p<0.001$), higher than the “vertical” mean in the flat environments ($t_{(32)}=5.07$, $p<0.0001$) and higher than the “horizontal” mean on the flat ($t_{(32)}=4.61$, $p<0.0001$). These findings arise because vertical translation mapped the stripes onto themselves, resulting in high mean correlation, whereas in all other conditions the translations progressively decorrelated the firing maps.

Nature Neuroscience: doi:10.1038/nn.2892

Helical track

Place cells

We analysed the upward and downward runs of 61 well-isolated CA1 place cells from 6 rats separately, totalling 103 place fields. The complete data set is shown in Supplementary figure 10 and Supplementary figure 12. From the real data we selected fields from coils at random to create 90 “dummy fields”, for comparative purposes.

Directionality

To the 42 cells that fired in both directions, we added another 17 for which one direction was excluded due to firing that was less than 50 spikes. These cells were considered to have rate remapped and were classified as directional. Out of 59 cells, then, 54 had a correlation between runs of less than 0.4 (or were considered rate remappers). Therefore, in line with previous work using linear tasks, the majority of cells in this study (92%) were directional.

Stability

Eight cells on upward runs and seven on downward runs from two rats were recorded over several days and analysed for stability. Inspection of the firing rate plots for these cells showed that, consistent with findings from studies of two-dimensional environments, the fields remained similar across trials. Statistical analysis confirmed that place fields on different trials were highly correlated with each other. The mean correlation (±s.e.m.) was 0.68 ± 0.06. Only 2 cells (13%) had correlation values below 0.4. Therefore, place cells on the helical track maintained stable fields over days. Actual peak locations were then compared using pairwise comparisons, which found an average

Nature Neuroscience: doi:10.1038/nn.2892

inter-peak distance across repeated trials of 0.83 coils. The simulations (where peaks were assigned to randomly chosen coils) were repeated 10000 times, producing a mean of 1.60 and standard deviation of 0.25; a value lower than 0.83 occurred only twice (probability of 0.0002). Therefore, peak locations in the real data were significantly more similar across trials than would be expected by chance, suggesting stability of the vertical place code.

Grid cells

We analysed the upward and downward runs of 27 grid cells separately, totalling 53 grid fields, from which we created 52 dummy grid fields.

Directionality

To assess directionality we compared the spatial and rate similarity between upward and downward runs. In total, we found 15 directional cells, 5 non-directional cells, and 6 cells that had a different classification on different trials. We then looked at cells recorded on one trial only, and found 15 directional and 3 non-directional cells. In both cases, the majority of cells are directional (58% vs. 83% respectively), in line with the place cells and with what has been reported previously for grid cells[10]. Note however that out of 7 cells recorded on multiple trials, the majority (71%) changed classification, from directional to non-directional, or vice versa. Examination of the place cell data found that out of 10 multiple-trial cells, none changed classification. This may reflect the generally higher variability of grid cell fields. This may be due to the greater number of subfields in grid cells; indeed, 4/6 grid cells displaying more than one subfield on the helix changed classification. The only single-field grid cell also changed classification, but only on the last two

Nature Neuroscience: doi:10.1038/nn.2892

out of 11 trials. Three of the five grid cells that changed classification were also unstable over several days in at least one direction, and 2 of these unstable cells had more than one subfield. Both cells that did not change classification were stable over days.

Stability

We next examined fields recorded on more than one trial. There were 10 fields in the upward direction and 8 in the downward direction. Again, the firing rate plots appear similar between trials. We calculated correlations between all pairs of trials and averaged them. The mean correlation was not as high as for place cells (0.50 ± 0.05 vs. 0.68 ± 0.06). However, the majority of fields were stable (67%). We found 6 fields below the user-defined cut-off point of 0.4 that were classified as non-stable across trials.

Actual peak locations were then compared using pairwise comparisons, which found an average inter-peak distance across repeated trials of 1.25 coils. The simulations (where peaks were assigned to randomly chosen coils) were repeated 10000 times, producing a mean of 1.60 and standard deviation of 0.19; a value lower than 1.25 occurred 275 times (probability of 0.03). Therefore, peak locations in the real data were significantly more similar across trials than would be expected by chance, suggesting, as for place cells (albeit more weakly), stability of the vertical place code.

Histology

The sites of the electrode tracks for the entorhinally implanted animals are plotted in Supplementary figure 13. Of the 10 implanted animals, 6 had electrode tracks verifiable as terminating in dorso-medial entorhinal cortex or

Nature Neuroscience: doi:10.1038/nn.2892

parasubiculum, while the tenth animal had electrodes apparently in the dentate molecular layer. Estimates sites from individual rats are detailed in the legend.

Nature Neuroscience: doi:10.1038/nn.2892